Monte Carlo calculations of the reflection electron energy loss spectra in gold

1997 J. Phys. D: Appl. Phys. 30 13

(http://iopscience.iop.org/0022-3727/30/1/003)

J. Phys. D: Appl. Phys. **30** (1997) 13–18. Printed in the UK PII: S0022-3727(97)73046-8

Monte Carlo calculations of the reflection electron energy loss spectra in gold

C M Kwei†‖, P Su†, Y F Chen‡ and C J Tung§

† Department of Electronics Engineering, National Chiao Tung University, Hsinchu, Taiwan
‡ Precision Instrument Development Center, Science-Based Industrial Park, Hsinchu, Taiwan
§ Department of Nuclear Science, National Tsing Hua University, Hsinchu, Taiwan

Received 25 March 1996

Abstract. The reflection electron energy loss spectra in gold have been calculated using a Monte Carlo approach. A description of Monte Carlo simulations based on the dielectric response theory for inelastic volume and surface excitations and the partial wave expansion method for elastic scattering was presented. The influence of surface excitations on the angular and energy spectra of reflected electrons was analysed. These excitations contributed to the energy spectra by single and plural inelastic loss peaks and by the multiple inelastic loss background. Surface plasmons were particularly important for glancing incident or escape electrons. The contribution from surface excitations to the angular spectra was significant for energy losses of a few tenths of an electronvolt but less significant for lower and higher energy losses. The angular spectra revealed single elastic scattering peaks for zero energy loss but flatter multiple elastic scattering curves for large energy losses. In all cases, Monte Carlo simulation results, including surface excitations, agreed very well with experimental data.

1. Introduction

Reflection electron energy loss spectroscopy (REELS) is a useful technique applied in surface and interface analyses [1, 2]. REELS makes use of the angular and energy spectra of electrons reflected from a solid surface by the incidence of fast electrons. The energy spectra provide information on inelastic interactions of electrons with the solid, which include single-electron ionizations and excitations (interband transitions), volume-plasmon excitations and surface-plasmon excitations. The angular spectra give data on elastic interactions of electrons with the solid atoms. Theoretical calculations of REELS may be carried out by a solution of the Boltzmann transport equation [3, 4] or by a simulation of the Monte Carlo (MC) method.

In most applications dealing with the transport equation, a multiple elastic scattering theory is applied [5, 6]. Expanding the angular distribution function in terms of the Legendre polynomial, it is able to solve the angular spectra by the so-called P_1-approximation [6]. A recent work [7] on elastic peak electron spectroscopy (EPES) has, however, shown that single and plural scatterings contribute significantly to the angular spectra of elastically backscattered electrons. Thus, multiple scattering theory is insufficient to describe the angular distribution of backscattered electrons. For the solution of energy spectra contributed by inelastic interactions, the transport equation may be solved by an iteration method [4]. This method, however, is useful only for small energy losses where few inelastic interactions are involved. A recent study [8] using x-ray photoelectron spectroscopy (XPS) has revealed that surface excitations made a significant contribution to the energy spectra in single and plural inelastic loss peaks and in multiple inelastic loss background. In order to obtain the full angular and energy spectra of REELS and to analyse the contribution from surface excitations, we have applied in this work MC simulations for REELS with and without surface excitations.

The accuracy of MC simulations depends on the modelling of interaction processes which include elastic scatterings, volume excitations (volume-plasmon excitations and interband transitions) and surface excitations. The basic inputs in MC calculations are elastic differential cross sections, differential inverse mean free paths (DIMFPs) for volume excitations, and differential probabilities for surface excitations. Here we applied the partial wave expansion method to estimate electron elastic differential cross sections using a Hartree–Fock–Winger–Seitz (HFWS) scat-

‖ To whom correspondence should be addressed. Tel: (886-35) 712121 ext. 54136. Fax: (886-35) 727300. E-mail address: cmkwei@cc.nctu.edu.tw

tering potential [9] for solid atoms. A finite difference technique [10] was employed to compute elastic scattering phase shifts. Electron DIMFPs for volume excitations and differential probabilities for surface excitations were estimated using a dielectric response theory [11,12]. Applying the sum rule constrained Drude dielectric function [13], we calculated these DIMFPs and differential probabilities for electrons of different energies and incidence and escape angles. Our model for surface excitations includes the recoil effect and abandons the small angle assumption. Owing to the difficulty in handling surface excitations in MC simulations, we applied a Poisson stochastic process for plural surface plasmon generations. In this work, we have calculated REELS in Au for electrons of moderately low energies and different incident and escape angles.

2. Theory

2.1. Monte Carlo simulations

MC simulations require a series of uniform random numbers to determine the path length, interaction type, energy loss, and scattering angle for each electron trajectory. Let a beam of monoenergetic electrons of energy E irradiate a semi-infinite solid with the interface surface on an xy plane. Let $+z$ be the surface normal directed inwardly into the solid. The number of surface plasmons, M, for an electron crossing a surface with angle α relative to the z-direction may be determined from

$$\sum_{n=0}^{M-1}\frac{1}{n!}[P_s(\alpha,E)]^n\exp[-P_s(\alpha,E)] < R_1 \leq \sum_{n=0}^{M}\frac{1}{n!}[P_s(\alpha,E)]^n\exp[-P_s(\alpha,E)] \tag{1}$$

where R_1 is a random number and α is either the incidence angle for impinging electrons, α_i, or the escape angle for emerging electrons, α_e. The electron probability for surface excitations, $P_s(\alpha, E)$, is given by

$$P_s(\alpha,E)=\int_0^E P_s(\alpha,E,\omega)\,\mathrm{d}\omega \tag{2}$$

where $P_s(\alpha, E, \omega)$ is the differential probability for surface excitations with the energy loss ω. The actual energy loss ω_s in each surface excitation is determined by another random number R_2 that satisfies

$$R_2=\frac{\int_0^{\omega_s}P_s(\alpha,E,\omega)\,\mathrm{d}\omega}{P_s(\alpha,E)}. \tag{3}$$

Applying Poisson statistics, the electron free path between two successive interactions s is determined by a third random number R_3 through

$$s=-\lambda_t\ln R_3 \tag{4}$$

where λ_t is the total (elastic and inelastic) mean free path of electrons. Let $\mu(E,\omega)$ be the DIMFP for volume excitations and $\mathrm{d}\sigma/\mathrm{d}\Omega$ be the elastic differential cross section. The corresponding inelastic and elastic mean free paths, λ_i and λ_e, are given by

$$\lambda_i^{-1}=\int_0^E\mu(E,\omega)\,\mathrm{d}\omega \tag{5}$$

and

$$\lambda_e^{-1}=N\int\frac{\mathrm{d}\sigma}{\mathrm{d}\Omega}\,\mathrm{d}\Omega \tag{6}$$

where N is the number of atoms per unit volume in the solid. Thus

$$\lambda_t^{-1}=\lambda_i^{-1}+\lambda_e^{-1}. \tag{7}$$

To determine whether an interaction is elastic or inelastic, a random number R_4 is generated. Satisfaction of the inequality

$$R_4\leq\frac{\lambda_e^{-1}}{\lambda_t^{-1}} \tag{8}$$

implies that an elastic interaction takes place. Otherwise, an inelastic interaction occurs. At each inelastic interaction, the actual energy loss ω_v is determined by the random number R_5 through

$$R_5=\lambda_i\int_0^{\omega_v}\mu(E,\omega)\,\mathrm{d}\omega. \tag{9}$$

The polar scattering angle θ at each elastic interaction is determined by the random number R_6 through

$$R_6=N\lambda_e\int_0^{\theta}\left(\frac{\mathrm{d}\sigma}{\mathrm{d}\Omega}\right)2\pi\sin\theta'\,\mathrm{d}\theta'. \tag{10}$$

In addition, the azimuthal angle ϕ is determined from

$$\phi=2\pi R_7 \tag{11}$$

using the random number R_7. Both θ and ϕ are angles relative to the electron direction before elastic scattering. The polar and azimuthal angles relative to the z-axis, i.e. Θ' and Φ', are given by

$$\cos\Theta'=\cos\Theta\cos\theta-\sin\Theta\sin\theta\cos\phi \tag{12}$$

$$\cos\Phi'=[\cos\Phi(\sin\theta\cos\phi\cos\Theta+\cos\theta\sin\Theta)-\sin\Phi\sin\theta\sin\phi][\sin\Theta']^{-1} \tag{13}$$

and

$$\sin\Phi'=[\sin\Phi(\sin\theta\cos\phi\cos\Theta+\cos\theta\sin\Theta)+\cos\Phi\sin\theta\sin\phi][\sin\Theta']^{-1} \tag{14}$$

where Θ and Φ are the polar and azimuthal angles relative to the z-axis of the electron before elastic scattering. The positional change of this electron after elastic scattering is then given by

$$\Delta x=s\sin\Theta'\cos\Phi' \tag{15}$$

$$\Delta y=s\sin\Theta'\sin\Phi' \tag{16}$$

and

$$\Delta z=s\cos\Theta'. \tag{17}$$

The trajectory of each electron is followed until either this electron is reflected back to the vacuum or its energy drops below the cut-off value.

2.2. Input data

The basic inputs in MC simulations are elastic differential cross sections, DIMFPs for volume excitations and differential probabilities for surface excitations. Previously, we have developed different models to calculate these quantities in applications of EPES [10] and XPS [8]. Our models involved the partial wave expansion method and the finite difference technique for elastic scatterings. A dielectric response theory involving the extended Drude dielectric function [13] was established for inelastic interactions. Both volume-plasmon and interband transition peaks in the energy loss function were identified and matched closely with experimental data. In addition, surface excitations were considered by including the recoil effect and abandoning the small angle assumption. A detailed description of these models is given elsewhere [10, 13]. Here we only present formulae necessary for the application in this work.

The elastic differential cross section for an electron of energy E is given in the partial wave expansion method as [14]

$$\frac{\mathrm{d}\sigma}{\mathrm{d}\Omega} = \frac{1}{8E}\left|\sum_{l=0}^{\infty}(2l+1)[\exp(2i\delta_l)-1]P_l(\cos\theta)\right|^2 \qquad (18)$$

where P_l is the Legendre polynomial of degree l and l is the orbital angular momentum quantum number. The phase shift δ_l can be calculated by a numerical solution of the radial Schrödinger equation. Applying a finite difference technique to the scattering potential derived from a HFWS electron density distribution, we can calculate the phase shifts and consequently elastic differential cross sections according to equation (18).

The DIMFP for volume excitations by an electron of energy E to lose energy ω is given by [11]

$$\mu(E,\omega) = \frac{1}{\pi E}\int_{q_-}^{q_+}\frac{\mathrm{d}q}{q}\,\mathrm{Im}\left[-\frac{1}{\varepsilon(q,\omega)}\right] \qquad (19)$$

where q is the momentum transfer, $q_\pm = \sqrt{2E} \pm \sqrt{2(E-\omega)}$ are derived from conservations of energy and momentum, and $\mathrm{Im}(-1/\varepsilon)$, i.e. the imaginary part of the negative inverse dielectric function, is the energy loss function. The dielectric function is given in the extended Drude model as a superposition of damped linear oscillators. Each oscillator is characterized by its own oscillator strength, damping coefficient and critical point energy. In the optical limit, i.e. $q \to 0$, the real and imaginary parts of the dielectric function may be expressed as

$$\varepsilon_1(0,\omega) = \varepsilon_b - \sum_{i=v}\frac{A_i[\omega^2-\omega_i^2]}{[\omega^2-\omega_i^2]^2+\omega^2\gamma_i^2} \qquad (20)$$

and

$$\varepsilon_2(0,\omega) = \sum_{i=v}\frac{A_i\gamma_i\omega}{[\omega^2-\omega_i^2]^2+\omega^2\gamma_i^2} \qquad (21)$$

where ε_b is a background dielectric constant due to the effect of polarizable ion cores and A_i, γ_i and ω_i are respectively the oscillator strength, damping coefficient, and critical point energy associated with the ith oscillator. Note that summations in equations (20) and (21) run, in general, over all valence electrons (denoted by the index v). In the case of Au, however, 5s and 5p inner electrons should also be included in these summations due to the strong overlapping of oscillator strengths between the valence band and these subshells in the vicinity of their binding energies [13]. Parameters in the extended Drude model can be determined by a fit of equation (20) to optical data and further verified by checking the constraints of sum rules [15]. The generalization of the optical dielectric function to the $q > 0$ region may be made by replacing ω_i in equations (20) and (21) by $\omega_i + k^2/2$ [16].

When an electron crosses a solid surface, it can excite surface-plasmons. The differential probability for surface excitations by an electron of energy E to cross a surface with angle α relative to the surface normal is given by

$$P_s(\alpha,E,\omega) = P_{s+}(\alpha,E,\omega) + P_{s-}(\alpha,E,\omega) \qquad (22)$$

where

$$P_{s\pm}(\alpha,E,\omega) = \frac{2}{\pi E\cos\alpha}\int_{q_-}^{q_+}\mathrm{d}q\,\frac{|q_s'|}{q^3}\,\mathrm{Im}\left[\frac{(\varepsilon-1)^2}{\varepsilon(\varepsilon+1)}\right] \qquad (23)$$

and

$$q_s' = \left[q^2 - \left(\frac{\omega+(q^2/2)}{\sqrt{2E}}\right)^2\right]^{1/2}\cos\alpha \pm \left(\frac{\omega+(q^2/2)}{\sqrt{2E}}\right)\sin\alpha. \qquad (24)$$

3. Results and discussion

Figure 1 shows a plot of elastic differential cross section as a function of scattering angle calculated using the partial wave expansion method and the finite difference technique. The full and broken curves are results corresponding to electrons of 2000 and 500 eV in Au. The fluctuations in these curves are due to the screening of nuclear charge by atomic electrons in different shells. This effect becomes larger for lower energy electrons because of their longer scattering time with the nucleus. At small scattering angles, or large impact parameters, the enhancement in screening makes the elastic differential cross section increase smoothly with reducing scattering angle. Figure 2 shows the inelastic DIMFP as a function of energy loss calculated using the extended Drude dielectric function for volume excitations. Representative results for electrons of 200, 500 and 1000 eV in Au are plotted. The sharp peaks in the curves are due to interband transitions of valence electrons. The broad peak at ~40 eV corresponds to the volume-plasmon excitation of valence electrons with a critical point energy of 38.5 eV [13]. A plot of differential probability for surface excitations by a 500 eV electron in Au is shown in figure 3 as a function of energy loss and crossing angle. It is seen that when the angle is large the differential probability exhibits a sharp maximum at ~2.5 eV. This maximum corresponds to the possibility of a surface-plasmon excitation. As the crossing angle decreases, the surface-plasmon peak broadens and lowers.

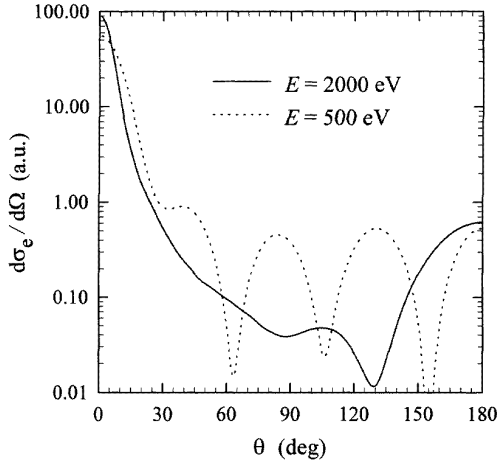

Figure 1. Elastic differential cross section as a function of scattering angle for electrons of several energies in Au. This cross section is expressed in atomic units.

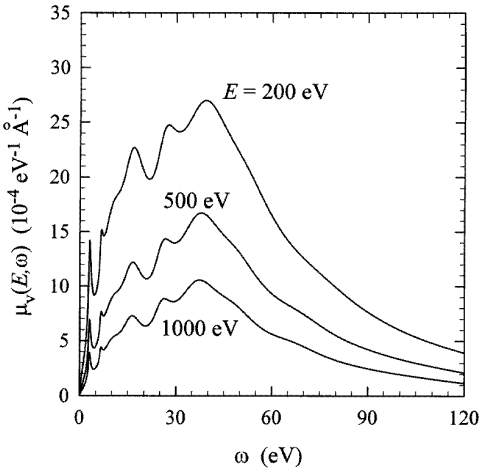

Figure 2. Inelastic DIMFP for volume excitations as a function of energy loss for electrons of several energies in Au.

This indicates that glancing electrons travelling longer path lengths near the surface have a greater probability to induce surface-plasmons.

REELS data of 1000 eV electrons impinging on a Au surface at 45° incidence angle and 75° escape angle are shown in figure 4. Here full curve represents experimental data [17]; the full and broken histograms are MC results including and neglecting the contribution from surface excitations respectively. Note that all spectra are normalized to the zero energy loss peak at the source energy. Further, the spectra are integral results over all azimuthal angles relative to the surface normal. In order to match the experimental conditions, we assume incident electrons to have a Gaussian distribution with 0.37% energy resolution. It is seen that MC results including surface excitations agree very well with experimental data. The contribution from surface excitations is significant both in single and plural loss peaks (near 1000 eV) and in a multiple loss background (far below 1000 eV). A similar plot of

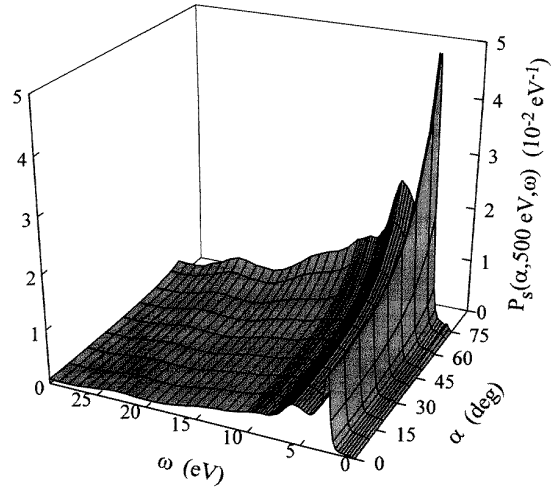

Figure 3. The differential probability for surface excitations as functions of energy loss and crossing angle (relative to the surface normal) for electrons of 500 eV impinging on or emerging from a Au surface.

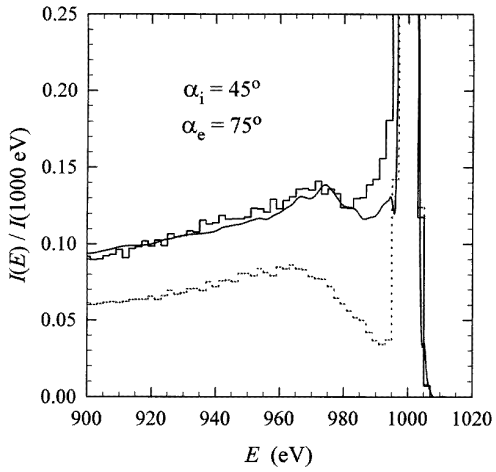

Figure 4. A comparison of energy spectra of REELS in Au for electrons of 1000 eV source energy, 45° incidence angle and 75° escape angle from experimental measurements (full curve) [17] and MC calculations with (full histogram) and without (broken histogram) surface excitations. Note that all results are normalized to the reflected electron intensity at the source energy.

REELS in Au is shown in figure 5 for 45° incidence angle and 0° escape angle. Here the contribution from surface excitations is less pronounced than that for a 75° escape angle. This reveals that glancing escape electrons have a greater probability of inducing surface excitations.

REELS data of 500 eV electrons impinging on a Au surface at 70° incidence angle are plotted in figures 6–8 as a function of scattering angle (relative to the impinging electron direction) for different energy losses. In all figures, the full curves represent experimental data [18] and full and broken histograms are MC results including and neglecting surface excitations respectively. To match the experimental conditions, we assume that velocities of incident and escape electrons lie on the same plane

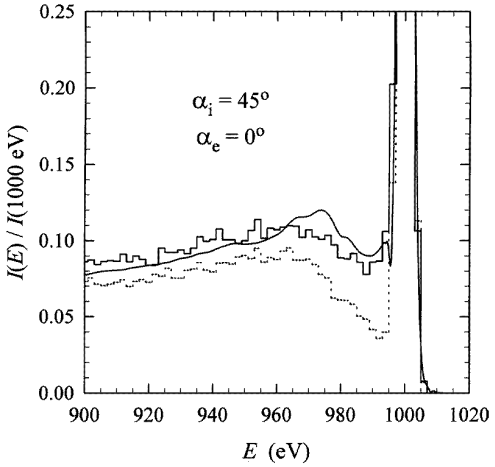

Figure 5. A comparison of energy spectra of REELS in Au for electrons of 1000 eV source energy, 45° incidence angle and 0° escape angle from experimental measurements (full curve) [17] and MC calculations with (full histogram) and without (broken histogram) surface excitations. Note that all results are normalized to the reflected electron intensity at the source energy.

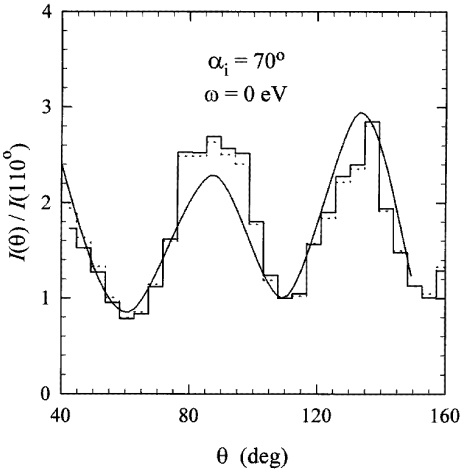

Figure 6. A comparison of angular spectra of REELS in Au for electrons of 500 eV source energy, 70° incidence angle and 0 eV energy loss from experimental measurements (full curve) [18] and MC calculations with (full histogram) and without (broken histogram) surface excitations. Note that all results are normalized to the reflected electron intensity at 110° scattering angle or 90° escape angle.

normal to the surface. Due to the inclined incidence, the scattering angle is asymmetric about the direction of incident electrons with respect to the surface geometry. Note that all spectra are normalized to the 110° scattering angle, i.e. 90° escape angle. Figure 6 shows that the angular spectra of reflected electrons with no energy loss exhibit structures close to those of the differential elastic cross section shown in figure 1. This indicates that single elastic scattering contributes significantly to the angular distribution of elastically reflected electrons. Indeed, the contribution from all plural and multiple elastic scatterings is less than that from single elastic scattering [7]. It can also be seen that the contribution from surface excitations is very small because no inelastic interaction actually occurs for zero energy loss. A comparison of figures 6–8 shows that the fluctuation in angular spectra becomes smaller for greater energy losses. This is because any fluctuation in the spectra is averaged out by the spread of electron energy in the case of increasing energy loss. In addition, a greater energy loss corresponds to an increased number of inelastic interactions. Thus, electrons travel deeper into the solid and are further attenuated. In the case of a 200 eV energy loss, the angular spectra seem to be symmetric about 110° scattering angle or 90° escape angle. This indicates that after many inelastic and elastic interactions deeply penetrating electrons lose their memory about the incident direction. On diffusion back to the surface [19], their angular distribution is nearly symmetric about the surface normal. Another comparison shows that the contribution from surface excitations is greater for an energy loss of 50 eV than for 0 eV but smaller for 100 eV than for 50 eV. Since each reflected electron crosses the surface only twice, one on its incidence and another on its escape, its total probability for surface excitation is therefore limited. Thus, the contribution from surface excitations to the angular spectra is smaller for an energy loss of 200 eV (of which a

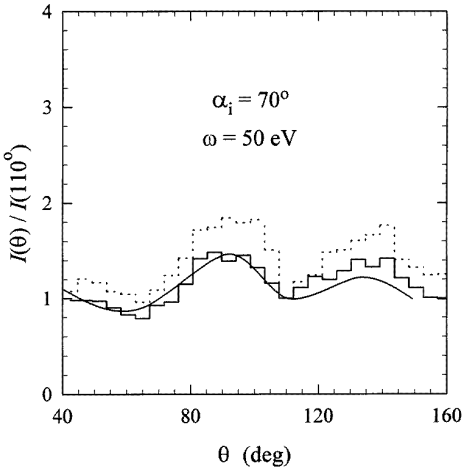

Figure 7. A comparison of angular spectra of REELS in Au for electrons of 500 eV source energy, 70° incidence angle and 50 eV energy loss from experimental measurements (full curve) [18] and MC calculations with (full histogram) and without (broken histogram) surface excitations. Note that all results are normalized to the reflected electron intensity at 110° scattering angle or 90° escape angle.

smaller part comes from surface excitations) than for 50 eV (a larger part comes from surface excitations). In all cases, MC simulations of REELS including surface excitations agree quite well with experimental data.

4. Conclusions

Monte Carlo simulations of REELS considering the contribution from surface excitations have never been performed. These simulations could provide information on the transport of electrons inside a solid and across a solid surface with respect to elastic scatterings, volume

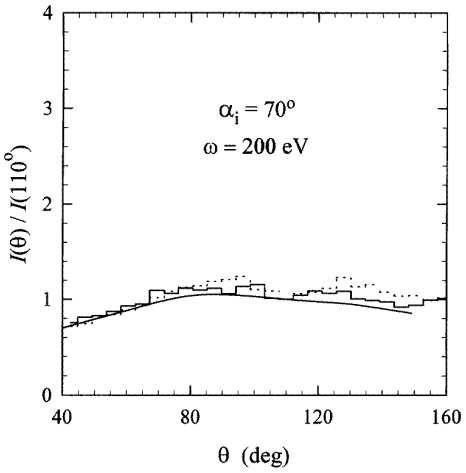

Figure 8. A comparison of angular spectra of REELS in Au for electrons of 500 eV source energy, 70° incidence angle and 200 eV energy loss from experimental measurements (full curve) [18] and MC calculations with (full histogram) and without (broken histogram) surface excitations. Note that all results are normalized to the reflected electron intensity at 110° scattering angle or 90° escape angle.

excitations and surface excitations. In this work, we have carried out these simulations for electrons of different energies, incidence angles and escape angles in Au. From analyses of the energy spectra it was found that the contribution from surface excitations is important in single and plural loss peaks and in multiple loss backgrounds. The contribution is particularly significant for escape electrons with glancing angles. From analyses of the angular spectra it was found that reflected electrons with no energy loss are contributed mainly by single elastic scatterings. In the case of a 200 eV energy loss, however, these electrons encountered many elastic and inelastic interactions so that their angular distribution was approximately symmetric about the surface normal. The contribution from surface excitations to the angular spectra was larger for an energy loss of 50 eV than for 0 eV but smaller for 100 eV than for 50 eV. This indicates that surface excitations contribute a smaller fraction to the energy loss as it became greater. In all cases, the simulated results including surface excitations agreed very well with experimental data.

Acknowledgment

This research was supported by the National Science Council of the Republic of China under Contract No NSC85-2215-E-009-060.

References

[1] Touggard S and Chorkendorff I 1987 *Phys. Rev.* B **35** 6570
[2] Touggard S and Kraaer J 1991 *Phys. Rev.* B **43** 1651
[3] Yubero F and Tougaard S 1992 *Phys. Rev.* B **46** 2486
[4] Tung C J, Chen Y F, Kwei C M and Chou T L 1994 *Phys. Rev.* B **49** 16 684
[5] Schiffing J S and Webb M B 1970 *Phys. Rev.* B **2** 1665
[6] Tofterup A L 1985 *Phys. Rev.* B **32** 2808
[7] Chen Y F, Kwei C M and Su P 1995 *J. Phys. D: Appl. Phys.* **28** 2163
[8] Wang J P, Tung C J, Chen Y F and Kwei C M 1996 *Nucl. Instrum. Methods* B **108** 331
[9] Tucker T C, Roberts L D, Nestor C W and Carson T A 1969 *Phys. Rev.* **178** 998
[10] Chen Y F, Su P, Kwei C M and Tung C J 1994 *Phys. Rev.* B **50** 17 547
[11] Egerton R F 1986 *Electron Energy Loss Spectroscopy in the Electron Microscope* (New York: Plenum)
[12] Tung C J and Ritchie R H 1977 *Phys. Rev.* B **16** 4302
[13] Kwei C M, Chen Y F, Tung C J and Wang J P 1993 *Surf. Sci.* **293** 202
[14] Jochain C J 1975 *Quantum Collision Theory* (Amsterdam: North-Holland)
[15] Chen Y F, Kwei C M and Tung C J 1993 *Phys. Rev.* B **48** 4373
[16] Ritchie R H, Hamm R N, Turner J E, Wright H A and Bolch W E 1991 *Physical and Chemical Mechanisms in Molecular Radiation Biology* ed W A Glass and M N Varma (New York: Plenum) p 99
[17] Yoshikawa H, Tsukamoto T, Shimizu R and Crist V 1992 *Surf. Interface Anal.* **18** 757
[18] Bronshtein I M, Pronin V P and Khinich I I 1981 *Sov. Phys. Solid State* **23** 349
[19] Tougaard S and Sigmund P 1982 *Phys. Rev.* B **25** 4452